JOURNAL OF Applied Polymer SCIENCE

Tensile Properties and Weibull Modulus of Some High-Performance Polymeric Fibers

Kimiyoshi Naito
National Institute for Materials Science, Environment and Energy Materials Division, Hybrid Materials Unit, Composite Materials Group, 1-2-1 Sengen, Tsukuba, Ibaraki 305-0047, Japan
Correspondence to: K. Naito (E-mail: naito.kimiyoshi@nims.go.jp)

ABSTRACT: The tensile properties and fracture behavior of poly-(*para*-phenylene-2,6-benzobisoxazole), poly-(*para*-phenylene terephthalamide), *co*-poly-(*para*-phenylene-3,4′-oxydiphenylene terephthalamide), polyarylate, polyethylene, and poly(lactic acid) high-performance polymeric fibers have been investigated. The Weibull statistical distributions of the tensile strength were also characterized. The results clearly show that for various types of high-performance polymer fibers, the Weibull modulus decreases with an increase in the tensile modulus, the tensile strength, and inverse of the failure strain. © 2012 Wiley Periodicals, Inc. J. Appl. Polym. Sci. 000: 000–000, 2012

KEYWORDS: fibers; mechanical properties; composites

Received 24 May 2012; accepted 1 August 2012; published online
DOI: 10.1002/app.38420

INTRODUCTION

Fibers are the basic load-bearing component in a fiber-reinforced composite. Reinforcing fibers used in modern composites can be broadly classified into three categories: (1) polymeric fibers, (2) carbon fibers, and (3) inorganic fibers.[1,2]

Carbon fibers are widely used as a reinforcement in composite materials because of their high-specific strength and modulus.[3] Currently, carbon fibers are derived from several precursors, with polyacrylonitrile (PAN) and pitch being the predominant precursor used today. The physical and mechanical properties of carbon fibers vary according to the precursor material and heat treatment conditions. PAN- and pitch-based carbon fibers generally have high strength, high modulus, and low density (1.6–2.2 g/cm^3).[4] Recently, the tensile, flexural properties, and Weibull modulus of ultrahigh strength PAN-based, ultrahigh modulus pitch-based, and high-ductility pitch-based single carbon fibers were characterized by Naito et al.[5–8]

Other interesting materials are polymeric fibers. The high-performance polymeric fibers exhibit high-tensile strength, modulus, and low density (0.9–1.6 g/cm^3), excellent strength to weight ratio, good dimensional stability, and enhanced thermal and chemical resistance.[9,10] High-performance polymeric fibers include extended fibers from rigid-rod isotropic crystal polymers [e.g., poly-(*para*-phenylene-2,6-benzobisoxazole) (PBO; e.g., Zylon)],[11,12] fibers from semiflexible isotropic crystal polymers such as poly(*para*-phenylene terephthalamide) (PPTA; e.g., Kevlar and Twaron),[13,14] and *co*-poly-(*para*-phenylene-3,4'-oxydiphenylene terephthalamide) (PPODTA; e.g., Technora),[15] thermotropic liquid-crystalline copolyester fibers (e.g., Vectran),[16] chain fibers from flexible polymers [e.g., Dyneema and Spectra fiber from ultrahigh molecular weight polyethylene (PE)],[17,18] and fibers from biodegradable polymers like poly(lactic acid) (PLA; e.g., Ecodear and Teramac).[19] There are three main routes to process these fibers: (i) a gel-spinning technology for PE fibers, (ii) a melt-spinning technology for thermotropic liquid crystalline copolyester fibers, and (iii) a dry-jet wet-spinning process for isotropic liquid crystalline polymer solutions. The evaluation of its mechanical property requires the knowledge of the mechanical characteristics of the fibers. Extensive work has been conducted to study the texture, morphology, mechanical, and thermal properties of high-performance polymeric fibers.[20–22]

In the present work, the tensile tests of single filaments for commercially available high-performance polymeric fibers were performed to evaluate the potential of them. Weibull statistical distributions on tensile strengths were also evaluated and tried to derive the deeper understanding of tensile properties of high-performance polymeric fibers.

EXPERIMENTAL

Materials

High-performance polymeric fibers used in this study were PBO fibers (ZylonAS, ZylonHS), PPTA fibers (Kevlar29, Kevlar49, Kevlar119, Kevlar129, Twaron), PPODTA fiber (Technora), polyarylate (PAR) fibers (VectranHT, VectranUM), PE fibers (Dyneema SK60, Dyneema SK71, Spectra900, Spectra1000,

Applied Polymer SCIENCE

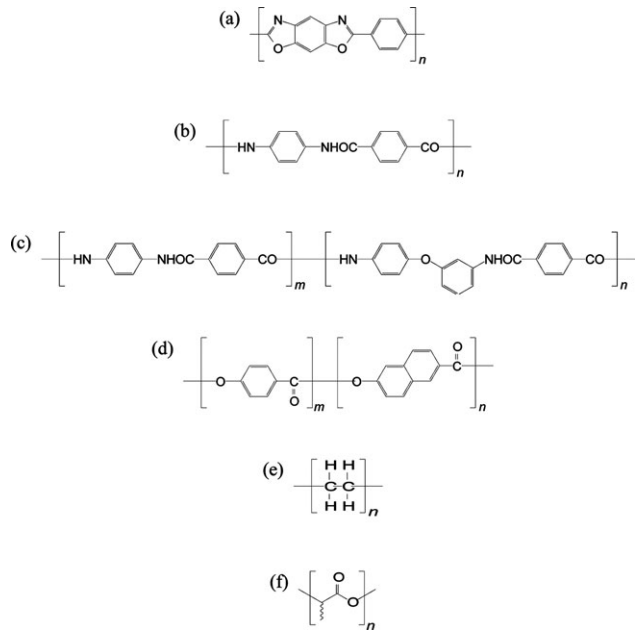

Figure 1. Chemical structures of various high-performance polymers. (a) Poly-(*para*-phenylene-2,6-benzobisoxazole) (PBO), (b) poly-(*para*-phenylene terephthalamide) (PPTA), (c) *co*-poly-(*para*-phenylene-3,4′-oxydiphenylene terephthalamide) (PPODTA), (d) polyarylate (PAR), (e) polyethylene (PE), and (f) poly(lactic acid) (PLA).

Spectra2000), and PLA fibers (Ecodear, Teramac). The Zylon and Dyneema fibers were supplied from Toyobo Co., Japan. The Kevlar fibers were supplied from DuPond-Toray Co., Japan. The Twaron/Technora fibers were supplied from Teijin Techno Products, Japan. The Vectran fibers were supplied from Kuraray Co., Japan. The Spectra fibers were supplied from Honeywell International, USA. The Ecodear fiber was supplied from Toray Industries, Inc., Japan, and the Teramac fiber was supplied from Unitika, Ltd., Japan. Chemical structures of high-performance polymeric fibers are shown in Figure 1 and the physical properties of these polymeric fibers are listed in Table I.

Specimen Preparation

Single filament polymeric fiber specimens were prepared on the stage with the help of a stereoscope. A single filament was selected from fiber bundles and cut perpendicular to the fiber axis by a razor blade. The diameter of the single polymeric fibers, d_f, was measured using a laser-scanning microscope (Lasertec Corp., Japan, 1LM15W) and a high-resolution scanning electron microscope (SEM; FEI Co., USA, Quanta 200FEG) at a low-vacuum mode of 100 Pa and an operating voltage of 7 kV before testing. The measured fiber diameters, d_f, are shown in Table I. All specimens were stored in a desiccator at 20°C ± 3°C and at 10% ± 5% relative humidity before testing.

Tensile Test

The tensile test of polymeric fibers was conducted based on ASTM C1557.[23] Tensile tests of single polymeric fibers were performed using a universal testing machine (Shimadzu Corp., Japan, Table top type tester EZ-Test) with a load cell of 10 N. The tensile specimen was prepared by fixing the filament on a paper holder with an instant cyanoacrylate adhesive, as reported elsewhere.[23,24] The specimen was set up to the testing machine. The holder was cut into two parts, before testing. The gauge length, L of 25 mm, and crosshead speed of 0.5 mm/min were applied. All tests were conducted under the laboratory environment at room temperature (at 23°C ± 3°C and 50% ± 5% relative humidity). Thirty specimens were tested for all polymeric fibers.

The tensile test gives a load, P as a function of extension, U^* curve up to failure. Tensile stress, σ, and tensile strain, ε, were calculated as follows:

$$\sigma = \frac{P}{\left(\frac{\pi d_f^2}{4}\right)} \tag{1}$$

$$\varepsilon = \frac{U^*}{L^*} \tag{2}$$

where L^* is a distance between targets (reference marks). The targets were marked on the fibers using the droplet types potted silver paste. The extension, U^*, was measured using a noncontact video extensometer (Shimadzu Corp., Japan, DVE-201). The DVE-201 extensometers performed precise, noncontact elongation measurements by using CCD cameras to capture digital images of test specimens. The tensile modulus, E_f, is calculated using a least-square method for the straight line section of stress–strain curve.

The fracture morphologies of these fibers were examined using a high-resolution SEM (FEI Co., USA, Quanta 200FEG) at a low-vacuum mode of 100 Pa and an operating voltage of 7 kV.

RESULTS AND DISCUSSION

Stress–Strain Relation

Figure 2 shows typical tensile stress–strain (σ–ε) curves for the PBO, PPTA, PPODTA, PAR, PE, and PLA high-performance polymeric fibers from single-fiber tensile testing. For the PBO (ZylonAS, ZylonHM) and the high-modulus PPTA (Kevlar49) fibers, the stress applied to the specimen is almost linearly proportional to the strain until failure. For the low-modulus PPTA (Kevlar29, Kevlar119, Kevlar129, Twaron), PPODTA (Technora), and PAR (VectranHT, VectranUM) fibers, the stress–strain curve shows slightly nonlinear behavior. The stress applied to the specimen is almost linearly proportional to the strain in the initial stage of loading (this modulus is defined as tensile modulus, E_f). Subsequently, the slope $d\sigma/d\varepsilon$ decreases slightly. Finally, the stress–strain curve of the fibers shows a clear slope increase as the deformation proceeds, thus indicating a cold-drawing process of the polymeric macromolecules during the tensile test. For the PE (Dyneema SK60, SK71, Spectra 900, 1000, 2000) fibers, the stress–strain curve is also shown nonlinear. The differences between the low-modulus PPTA, PPODTA, PAR fibers, and the PE fibers are the slope ($d\sigma/d\varepsilon$) behaviors. The stress–strain curve of the PE fibers shows a clear slope decrease as the deformation proceeds and especially for the Spectra 900 and 1000 fibers, the stress gradually decreases with increasing the strain after the stress reaches the maximum value. For the PLA (Ecodear, Teramac) fibers, the stress–strain curve shows large

Table I. Physical and Mechanical Properties of High-Performance Polymeric Fibers

	PBO		PPTA					PPODTA	PAR		PE					PLA	
	ZylonAS	ZylonHS	Kevlar29	Kevlar49	Kevlar119	Kevlar129	Twaron	Technora	VectranHT	VectranUM	Dyneema SK60	Dyneema SK71	Spectra 900	Spectra 1000	Spectra 2000	Ecodear	Teramac
Fiber	ZylonAS A555T332 813RD	ZylonHS A3270T1992 H12RD	Kevlar29 1670T/ 956	Kevlar49 1270T/ 968	Kevlar119 1670T/ 956E	Kevlar129 1670T/ 956C	Twaron 1680T1000 T1000	Technora 1670T1000 T741	VectranHT 1670T600 T101M	VectranUM 1580T200 T101	SK60 220T192 410	SK71 220T192 410HN	S900 1200/120	S1000 650/120	S2000 180/60 AE	Ecodear 33T10	Teramac 1100T140 P17
Supplier	Toyobo Co., Ltd.		DuPont-Toray Co., Ltd.				Teijin Techno Products, Ltd.		Kuraray Co., Ltd.		Toyobo Co., Ltd.		Honeywell International, Inc.			Toray Industries, Inc.	Unitika, Ltd.
Filaments (Count)[a]	332	1992	956	968	956	956	1000	1000	600	200	192	192	120	120	60	10	140
Dtex (g/10,000 m)[a]	555	3270	1670	1270	1670	1670	1680	1670	1670	1580	220	220	1333	722	200	33	1100
Density ρ (g/cm^3)[a]	1.54	1.56	1.44	1.45	1.44	1.44	1.44	1.39	1.41	1.41	0.97	0.97	0.97	0.97	0.97	1.27	1.27
Average tensile modulus $E_{f.ave}$ (GPa)[b]	184.5 (12.9)	235.8 (12.8)	85.3 (5.9)	149.1 (12.3)	61.4 (5.3)	99.0 (8.1)	77.9 (5.8)	85.7 (6.8)	82.1 (14.3)	104.7 (7.0)	71.6 (7.4)	107.9 (12.7)	54.0 (4.2)	85.4 (10.6)	128.5 (17.1)	5.88 (0.31)	8.69 (0.56)
Average tensile strength $\sigma_{f.ave}$ (GPa)[b]	5.49 (0.78)	5.35 (0.73)	3.30 (0.31)	3.85 (0.52)	2.97 (0.27)	3.27 (0.35)	3.28 (0.33)	3.45 (0.29)	4.23 (0.39)	4.12 (0.48)	2.60 (0.25)	3.22 (0.32)	2.18 (0.15)	2.71 (0.21)	3.26 (0.34)	0.23 (0.01)	0.41 (0.03)
Average failure strain $\varepsilon_{f.ave}$ (%)[b]	3.06 (0.31)	2.41 (0.31)	3.68 (0.22)	2.45 (0.28)	3.97 (0.27)	3.33 (0.31)	3.77 (0.22)	4.19 (0.30)	3.43 (0.18)	3.06 (0.27)	3.90 (0.41)	3.69 (0.43)	7.61 (1.40)	6.89 (1.97)	4.60 (0.62)	40.9 (5.6)	29.8 (1.3)
Weibull modulus m_f	7.8	7.4	11.8	8.2	11.8	10.3	10.6	13.2	11.9	9.4	11.3	11.0	15.2	13.3	10.0	18.2	17.3
Diameter d_f (μm)[b]	11.06 (0.61)	10.95 (0.87)	13.79 (0.99)	10.27 (0.78)	10.92 (0.77)	11.58 (0.95)	12.82 (0.69)	12.74 (0.64)	15.66 (1.42)	24.12 (1.55)	12.74 (0.89)	12.75 (1.29)	39.83 (3.43)	30.23 (3.48)	23.76 (1.44)	14.81 (0.62)	24.05 (1.45)

[a]Producer's data sheet ZylonAS and HS: Catalog for PBO Fiber Zylon, Toyobo Co., Ltd., 2005. Kevlar29, 49, 119, and 129: Catalog for DuPont Kevlar, DuPont-Toray Co., Ltd., 2008. Twaron: Catalog for Twaron, Teijin Techno Products, Ltd., 2009. Technora: Catalog for High-Strength Aramid Fiber Technola, Teijin Techno Products, Ltd., 2009. VectranHT and UM: Catalog for Vectran, Kuraray Co. Ltd., 2006. Dyneema SK60 and SK71: Catalog for Dyneema, Toyobo Co., Ltd., 2009. Spectra900, 1000, and 2000: Catalog for High-strength, Light-weight Polyethylene Fiber, Honeywell International, Inc., 2007. Ecodear: Catalog for PLA Fiber Ecodear, Toray Industries, Inc., 2009. Teramac: Catalog for PLA Fiber Teramac, Unitika, Ltd., 2000.

[b]() Indicate standard deviations.

Applied Polymer SCIENCE

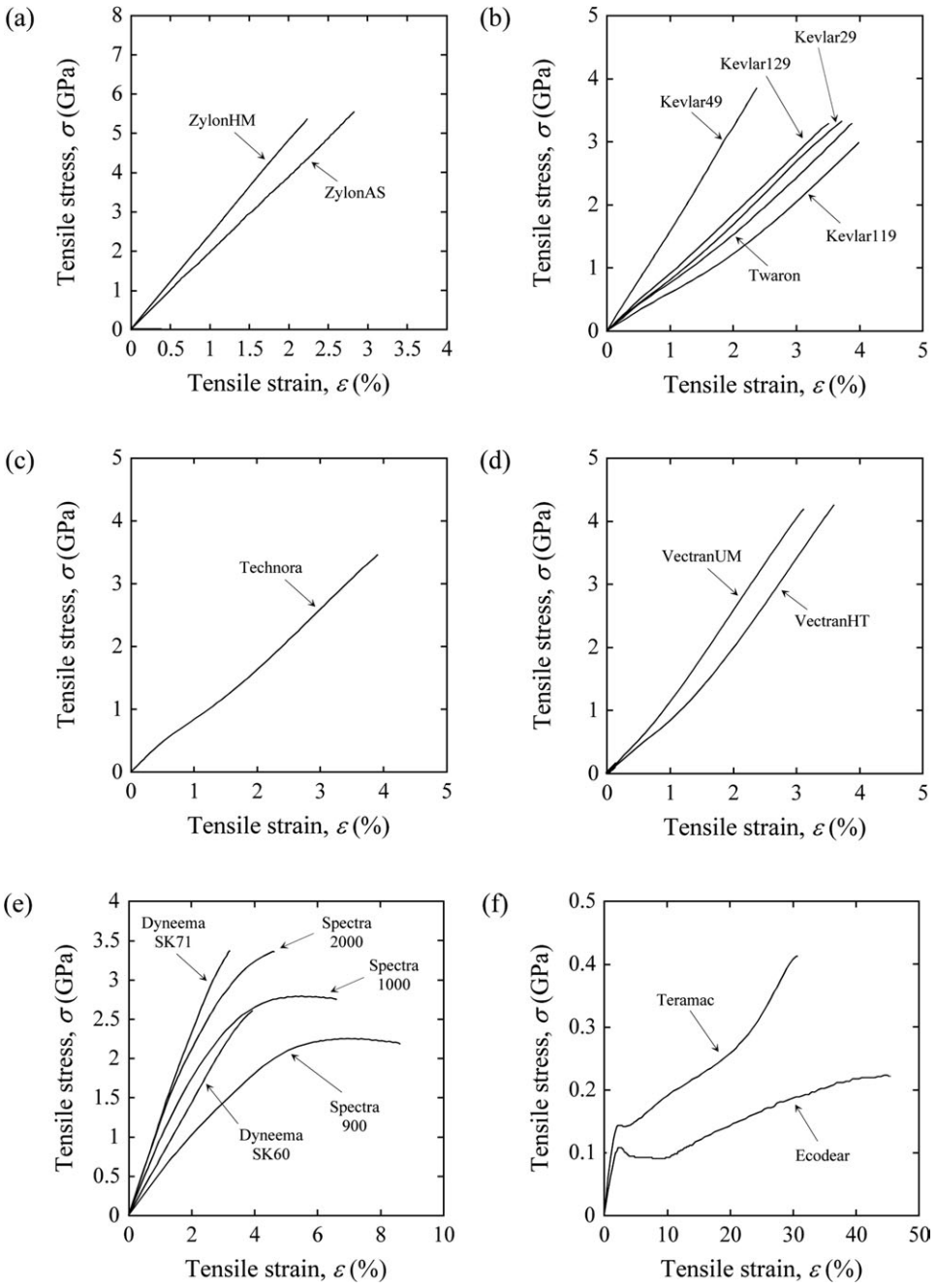

Figure 2. Typical tensile stress–strain curves for the PBO, PPTA, PPODTA, PAR, PE, and PLA high-performance polymeric fibers. (a) PBO fibers, (b) PPTA fibers, (c) PPODTA fiber, (d) PAR fibers, (e) PE fibers, and (f) PLA fibers.

nonlinear behavior and complicated shape. The stress applied to the specimen is almost linearly proportional to the strain in the initial stage of loading (this modulus is defined as tensile modulus, E_f). Then the curve becomes nonlinear and the stress reaches maximum. Subsequently, the stress gradually decreases with increasing the strain, and the fibers hold a stress value. Finally, the fibers continue to increase the stress and the strain showing the large nonlinear behavior without instantaneous failure.

The difference in the stress–strain curves among the high-performance polymeric fibers strongly depends on the crystallinity and preferential orientation of the fibril structures, although the absolute tensile modulus and strengths of the fibers depend on the character of materials (molecular structures, weights, etc.). For the highly crystallinity and oriented fibril structures of the PBO (ZylonAS, ZylonHM) and the PPTA (Kevlar49) fibers,[20] which is observed in the tensile modulus of fibers, the stress–strain curve shows almost linear behavior. For the highly crystallinity and slightly curved fibril structures of the PPTA (Kevlar29, Kevlar119, Kevlar129, Twaron), PPODTA (Technora), and PAR (VectranHT, VectranUM) fibers, the stress–strain curve shows almost linear behavior in the initial stage of loading. The curvature structures change to line-oriented structures with

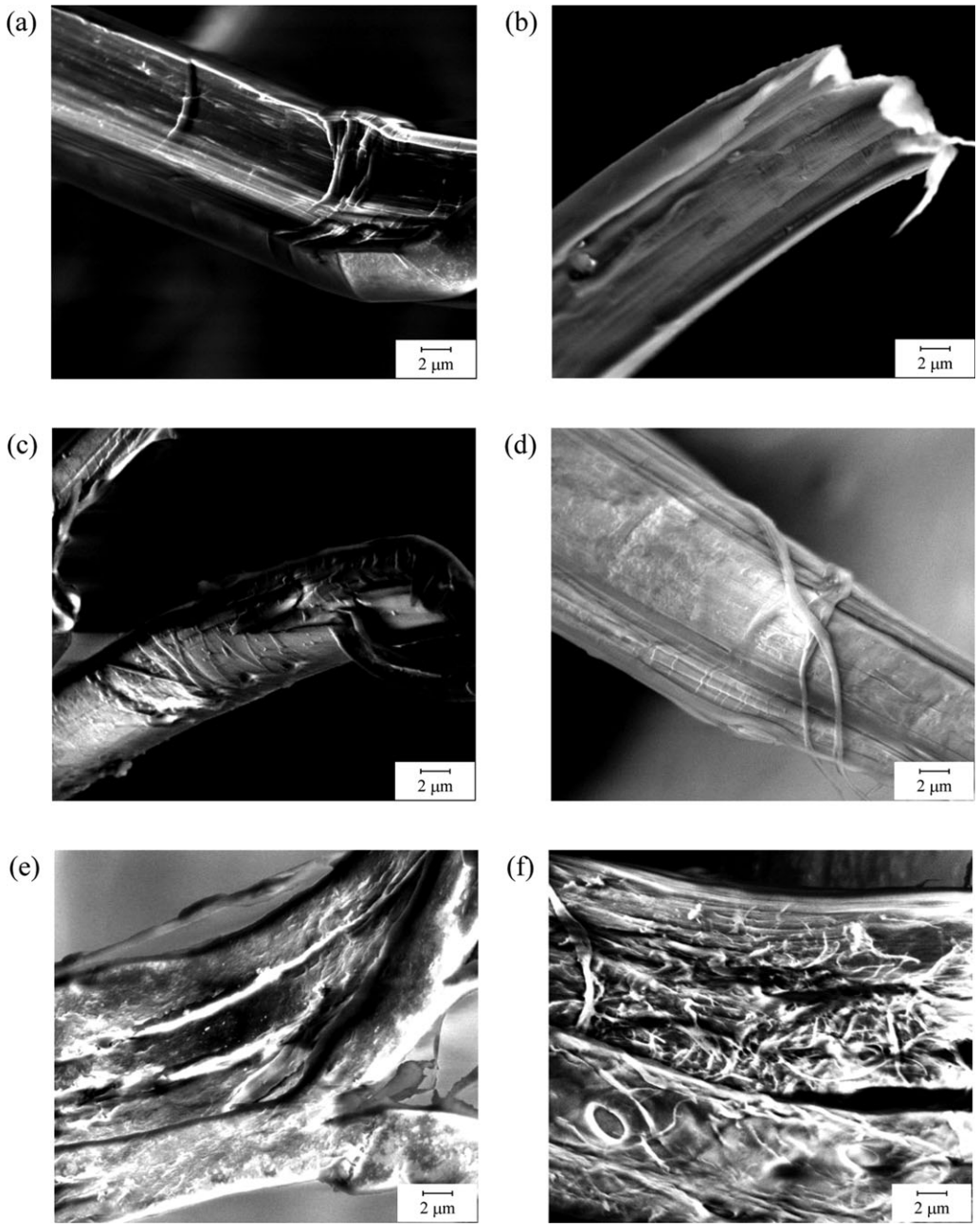

Figure 3. SEM micrographs of the tensile fractured surfaces showing the transverse cross-section structure of the PBO (ZylonAS), PPTA (Kevlar29), PPODTA (Technora), PAR (VectranHT), PE (Dyneema SK60), and PLA (Ecodear) high-performance polymeric fibers. (a) PBO (ZylonAS) fiber, (b) PPTA (Kevlar29) fiber, (c) PPODTA (Technora) fiber, (d) PAR (VectranHT) fiber, (e) PE (Dyneema SK60) fiber, and (f) PLA (Ecodear) fiber.

increase in loading. Finally, the estimated modulus (the slope $d\sigma/d\varepsilon$) increases as the deformation proceeds. For the relatively low crystallinity and highly oriented fibril structures of the PE (Dyneema SK60, SK71, Spectra 900, 1000, 2000) fibers,[20] the stress–strain curve shows almost linear behavior in the initial stage of loading. Subsequently, the estimated modulus (the slope $d\sigma/d\varepsilon$) decreases as the deformation proceeds due to the lower crystallinity of fibers. The tensile strengths of the PBO, PPTA, PPODTA, PAR, and PE polymeric fibers showed high values (more than 2 GPa), which were almost similar to those of carbon fibers, and the failure strains of these polymeric fibers also showed high values (more than 2%), which were higher than those of carbon fibers (less than 2%). In addition, the tensile responses of these fibers showed linear behaviors in the initial stage of loading. It was easy to design the strength criterion, and these fibers are one of the best load-bearing components in a polymeric fiber reinforced composite, although it is important to consider the interfacial shear strength between the fibers and the matrices. For the crystalline and amorphous form stacked within the microfibrils and the interfibrillar structures PLA (Ecodear, Teramac) fibers,[22] by the crystalline and amorphous fibrils, the fiber shows the intermediate modulus in

Applied Polymer SCIENCE

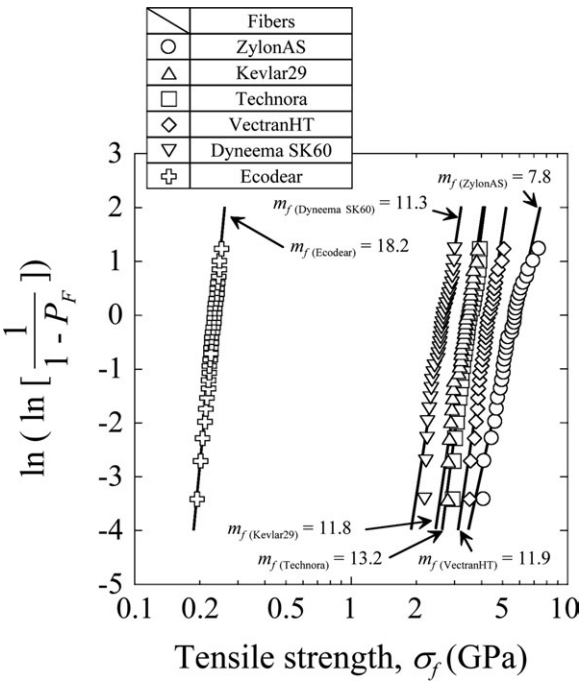

Figure 4. Weibull plots for the PBO (ZylonAS), PPTA (Kevlar29), PPODTA (Technora), PAR (VectranHT), PE (Dyneema SK60), and PLA (Ecodear) high-performance polymeric fibers.

the initial stage of loading. Subsequently, when a weak fibril begin to fail and delamination occurs between fibrils, the high-elongated amorphous fibrils would hold the load (strength), and the stress–strain curve shows large nonlinear behavior and complicated shape. The tensile responses of the PLA fibers were interesting and effective to use the safety reason, because these fibers did not show a catastrophic failure. However, the tensile strengths of these fibers were quite low, and it is important to enhance the tensile strengths of these fibers in order to use the structural components.

Tensile Modulus, Strength, and Failure Strain

The average tensile modulus ($E_{f.ave}$), strength ($\sigma_{f.ave}$), and failure strain ($\varepsilon_{f.ave}$) were summarized in Table I. The measured modulus, strength, and strain of these fibers were almost similar to that in each product data. The results showed that the PBO (ZylonAS, ZylonHM) and high-modulus PPTA (K49) fibers have the average tensile strength, $\sigma_{f.ave}$ of 5.49 ± 0.78 (ZylonAS), 5.35 ± 0.73 (ZylonHM), and 3.85 GPa ± 0.52 GPa (Kevlar49), and the average tensile modulus, $E_{f.ave}$ of 184.5 ± 12.9 (ZylonAS), 235.8 ± 12.8 (ZylonHM), and 149.1 GPa ± 12.3 GPa (Kevlar49). The PLA (Ecodear, Teramac) fibers have the average failure strain, $\varepsilon_{f.ave}$ of 40.9 ± 5.6 (Ecodear) and 29.8% ± 1.3% (Teramac) although the tensile modulus and strength are quite low. The low-modulus PPTA (Kevlar29, Kevlar119, Kevlar129, Twaron), PPODTA (Technora), PAR (VectranHT, VectranUM), and PE (Dyneema SK60, SK71) fibers have the average tensile modulus, $E_{f.ave}$ ranging from 54.0 to 128.5 GPa, the average tensile strength, $\sigma_{f.ave}$ ranging from 2.18 to 4.23 GPa, and the average failure strain, $\varepsilon_{f.ave}$ ranging from 3.06 to 7.61%, respectively.

Fracture Morphology

SEM micrographs of transverse cross-sectional views for the tensile fractured surfaces of the PBO (ZylonAS), PPTA (Kevlar29), PPODTA (Technora), PAR (VectranHT), PE (Dyneema SK60), and PLA (Ecodear) high-performance polymeric fibers are shown in Figure 3. The high-performance polymeric fibers have fibrillar structures. For the PBO fiber, the elongated microvoid structure on the fibrils was seen. For the PPTA and PPODTA fibers, a lot of nanosize transverse cracks were observed in the fibrils. For the PAR fiber, a lot of nanosize dimples were observed in the fibrils. For the PE fiber, a lot of dimples were also observed in the fibrils, and the size was larger than that of the PAR fiber. For PLA fiber, the highly oriented fibrils and nonoriented fibrils were clearly observed. Further structural discussions and structural modeling were observed in the literature.[20,22] The longitudinal splitting fracture morphologies were observed because of the extreme anisotropy in high-

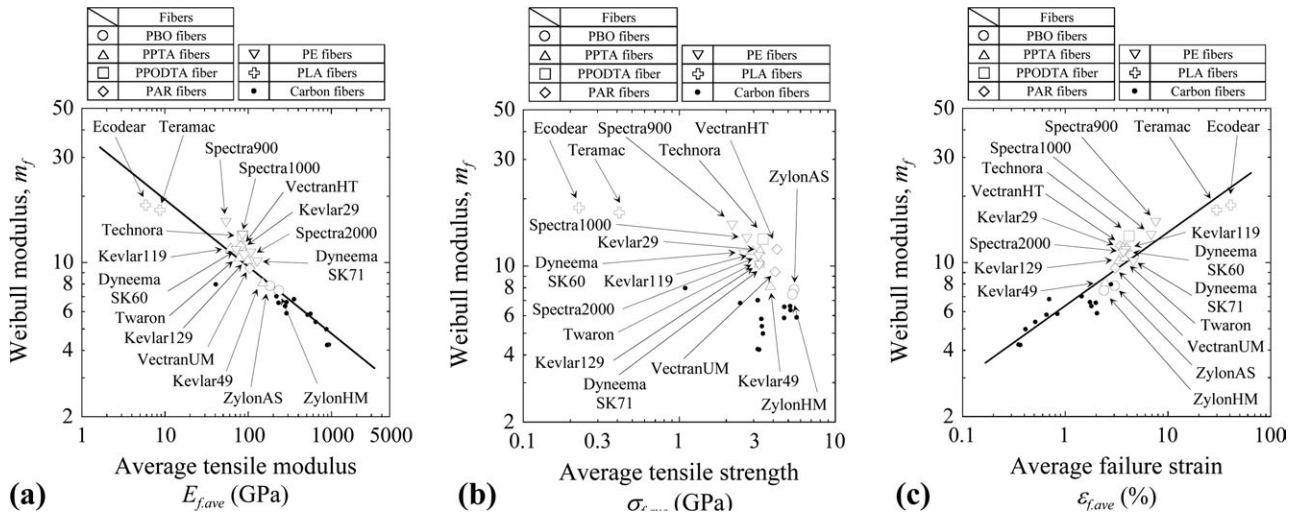

Figure 5. Weibull modulus of the PBO, PPTA, PPODTA, PAR, PE, and PLA polymeric fibers as a function of the average tensile modulus, the average tensile strength, and the average failure strain. (a) tensile modulus, (b) tensile strength, and (c) failure strain.

performance polymeric fibers. Similar splitting morphologies were observed in the anisotropy high-modulus pitch-based carbon fibers, although the pitch-based carbon fibers have graphite crystallite sheet-like morphology, and the graphite sheets are a result of pull out at failure.[4,5] Transverse and shear strength of the high-performance polymeric fibers, as well as the pitch-based carbon fibers, were quite low, and the compressive strength of these fibers became lower. It is necessary to consider these advantages and disadvantages (the interfacial shear strengths between the fibers and the matrices were also important) for applications.

Weibull Modulus

The results shown in Table I clearly indicate that there is an appreciable scattering of tensile strength. The statistical distribution of fiber tensile strengths is usually described by means of the Weibull equation.[25,26] The two-parameter Weibull distribution is given by

$$P_F = 1 - \exp\left[-L\left(\frac{\sigma_f}{\sigma_0}\right)^{m_f}\right] \tag{3}$$

where P_F is the cumulative probability of failure of a fiber of length L at applied tensile strength σ_f, m_f is the Weibull modulus (Weibull shape parameter) of the fiber, and σ_0 is a Weibull scale parameter (characteristic stress). The cumulative probability of failure, P_F, under a particular stress is given by

$$P_F = \frac{i}{n+1} \tag{4}$$

where i is the number of fibers that have broken at or below a stress level and n is the total number of fibers tested. Rearrangement of eq. (3) gives the following:

$$\ln\left(\ln\left[\frac{1}{1-P_F}\right]\right) = m_f \ln(\sigma_f) - m_f \ln\left(\sigma_0 L^{1/m_f}\right) \tag{5}$$

Hence the Weibull modulus, m_f, can be obtained by linear regression from a Weibull plot of eq. (5).

Figure 4 shows the Weibull plots of the PBO (ZylonAS), PPTA (Kevlar29), PPODTA (Technora), PAR (VectranHT), PE (Dyneema SK60), and PLA (Ecodear) high-performance polymeric fibers. The Weibull modulus, m_f, for the PBO (ZylonAS), PPTA (Kevlar29), PPODTA (Technora), PAR (VectranHT), PE (Dyneema SK60), and PLA (Ecodear) fibers was calculated to be 7.8, 11.8, 13.2, 11.9, 11.3, and 18.2, respectively. The Weibull modulus (m_f) was also summarized in Table I. The results clearly show that high-modulus PBO polymeric fibers has the low-Weibull modulus, m_f, and failure strain, ε_f, while the high-ductility PLA polymeric fiber has the high-Weibull modulus, m_f, and failure strain, ε_f.

In the previous investigation,[8] the relationship between the Weibull modulus and the average tensile strength was evaluated on log–log scale, and it was found that there was a linear relation between the Weibull modulus and the average tensile strength, while this investigation examined the effect of gauge length on the tensile strength and the Weibull modulus of several types of carbon fibers. In the study, the relationships between the Weibull modulus and the tensile modulus, strength, and failure strain were also evaluated on log–log scale.

Figure 5 is a representation of the Weibull modulus, m_f, as a function of the average tensile modulus, $E_{f.ave}$, the average tensile strength, $\sigma_{f.ave}$, and the average failure strain, $\varepsilon_{f.ave}$, for the PBO, PPTA, PPODTA, PAR, PE, and PLA polymeric fibers. The results for the high-strength PAN-based (T1000GB, T800HB, T700SC, T300, and IM600), high-modulus PAN-based (M60JB, M40B, and UM55), high-modulus pitch-based (K13D, K13C, K135, and XN-90), and high-ductility pitch-based (XN-05) carbon fibers at same gauge length (25 mm) are also shown in this figure.[5,7] From the viewpoints of the Weibull modulus distribution, it can be seen that for the PBO, PPTA, PPODTA, PAR, PE, PLA polymeric fibers, and the PAN- and pitch-based carbon fibers, the Weibull modulus, m_f, decreases with an increase in the average tensile modulus, $E_{f.ave}$, the average tensile strength, $\sigma_{f.ave}$, and a decrease in the average failure strain, $\varepsilon_{f.ave}$. In addition, there is an almost linear relation between the tensile modulus, failure strain, and the Weibull modulus on log–log scale.

The Weibull modulus relates to the strength distribution and the tensile modulus relate to flaw sensitivity, although the absolute tensile modulus and strengths of the fibers depend on the character of materials (molecular structures, weights, crystallinity, preferential orientation, etc.). This relationship indicates that the tensile strength distribution of fibers strongly depend on the flaw sensitivity (tensile modulus) and is clearly observed in Figure 5(a). For example, the higher tensile moduli of fibers become wider distributions of tensile strength. Similarly, the higher tensile strengths and lower failure strains become wider distributions of tensile strength. Especially, the Weibull modulus strongly depend on the failure strain, as shown in Figure 5(c), because the tensile responses of the polymeric fibers show nonlinear behaviors, and the fracture process is a ductile nature. The average failure strain, $\varepsilon_{f.ave}$, is a useful parameter to illustrate differences in the tensile properties, including the Weibull modulus.

Fibers are the basic load-bearing component in a fiber-reinforced composite. The Weibull modulus of tensile strengths for single fibers (as well as the tensile modulus, strength, and failure strain of single fibers) usually depend on that for fiber-reinforced composites, although the interfacial shear strengths between the fibers and the matrices also depend on the tensile modulus, strength, failure strain, and Weibull modulus of the fiber-reinforced composites. It is considered that these relationships, as shown in Figure 5, are useful for the first material selection.

CONCLUSIONS

The tensile properties and fracture behavior of PBO, PPTA, PPODTA, PAR, PE, and PLA high-performance polymeric fibers have been investigated. The Weibull statistical distributions of the tensile strength for the PBO, PPTA, PPODTA, PAR, PE, and PLA high-performance polymeric fibers were also characterized. The results are briefly summarized:

1. For the PBO and the high-modulus PPTA fibers, the stress was almost linearly proportional to the strain until failure. However, for the low-modulus PPTA, PPODTA, PAR, and PE fibers, the stress–strain curve was slightly nonlinear and for the PLA fibers, and the stress–strain curve showed large nonlinear behavior and complicated shape.
2. The Weibull modulus of all polymeric fibers was calculated to be ranging from 7.4 to 18.2. The results clearly show that the high-modulus PBO (ZylonHM) polymeric fiber has the lowest Weibull modulus and failure strain, while the high-ductility PLA (Ecodear) polymeric fiber has the highest Weibull modulus and failure strain.
3. For each type of polymeric fiber, the Weibull modulus decreases with an increase in the tensile modulus, the tensile strength, and decrease in the failure strain.

REFERENCES

1. Watt, W.; Perov, B. V. Handbook of Composites, Vol. 1: Strong Fiber; North-Holland: New York, **1985.**
2. Bunsell, A. R. In Composite Materials Series, Vol. 2: Fibre Reinforcements for Composite Materials; Bunsell, A. R., Ed.; Elsevier: New York, **1988;** pp 1–17.
3. Chand, S. *J. Mater. Sci.* **2000,** *35*, 1303.
4. Morgan, P. Carbon Fibers and Their Composites; Taylor & Francis: New York, **2005.**
5. Naito, K.; Tanaka, Y.; Yang, J. M.; Kagawa, Y. *Carbon* **2008,** *46*, 189.
6. Naito, K.; Tanaka, Y.; Yang, J. M.; Kagawa, Y. *J. Am. Ceram. Soc.* **2009,** *92*, 186.
7. Naito, K. In Impregnation Improvement and Reliability Evaluation for CFRP (in Japanese); Takahashi, A., Ed.; Technical Information Institute Co. Ltd.: Tokyo, **2010;** pp 34–46.
8. Naito, K.; Yang, J. M.; Tanaka, Y.; Kagawa, Y. *J. Mater. Sci.* **2012,** *47*, 632.
9. Kumar, S.; Wang, Y. In Composite Engineering Handbook; Mallick, P. K., Ed.; Marcel Dekker: New York, **1997;** pp 51–100.
10. Hersh, S. P. In Handbook of Fiber Science and Technology, Vol. III: High Technology Fibers Part A; Lewin, M.; Preston, B. V., Eds.; Marcel Dekker: New York, **1985;** pp 1–50.
11. Marder, E.; Melcher, S.; Liu, J. W.; Gao, S. L.; Bianchi, A. D.; Zherlitsyn, S.; Wosnitza, J. *J. Mater. Sci.* **2007,** *42*, 8047.
12. Horikawa, N.; Nomura, Y.; Kitagawa, T.; Haruyama, Y.; Sakaida, A.; Imamichi, T.; Sasaki, S.; Fukaya, T. *J. Soc. Mater. Sci. Jpn.* **2008,** *57*, 732.
13. Rao, Y.; Waddon, A. J.; Farris, R. *J. Polymer* **2001,** *42*, 5937.
14. Languerand, D. L.; Zhang, H.; Murthy, N. S.; Ramesh, K. T.; Sansoz, F. *Mater. Sci. Eng. A-Struct.* **2009,** *500*, 216.
15. Wu, T. M.; Blackwell, J. *Macromolecules* **1996,** *29*, 5621.
16. Pegoretti, A.; Zanolli, A.; Migliaresi, C. *Compos. Sci. Technol.* **2006,** *66*, 1970.
17. Xu, T.; Farris, R. *J. Polym. Eng. Sci.* **2007,** *47*, 1544.
18. Hine, P. J.; Ward, I. M.; Jordan, N. D.; Olley, R. H.; Bassett, D. C. *J. Macromol. Sci. B.* **2001,** *40*, 959.
19. Lim, L. T.; Auras, R.; Rubino, M. *Prog. Polym. Sci.* **2008,** *33*, 820.
20. Afshari, M.; Sikkema, D. J.; Lee, K.; Bogle, M. *Polym. Rev.* **2008,** *48*, 230.
21. Sikkema, D. J.; Northolt, M. G.; Pourdeyhimi, B. *MRS Bull.* **2003,** *28*, 579.
22. Gupta, B.; Revagade, N.; Hilborn, J. *Prog. Polym. Sci.* **2007,** *32*, 455.
23. ASTM C1557-03 Standard Test Method for Tensile Strength and Young's Modulus of Fibers; American Society for Testing and Materials: West Conshohocken, PA., 2008; ASTM Annual Book of Standards, Vol. 15.01.
24. Sung, M. G.; Sassa, K.; Tagawa, T.; Miyata, T.; Ogawa, H.; Doyama, M.; Yamada, S.; Asai, S. *Carbon* **2002,** *40*, 2013.
25. Weibull, W. *J. Appl. Mech.* **1951,** *18*, 293.
26. van der Zwaag, S. *J. Test. Eval.* **1989,** *17*, 292.